First demonstration of a non-orthogonal Lloyd's mirror interferometer with a spatial light modulator for arbitrary two-dimensional pattern fabrication

NOZOMU TAKAHIRO,[1] YUKI SHIMIZU[1,*]

[1]*Division of Mechanical and Aerospace Engineering, Hokkaido University, N13W8 Kita-ku, Sapporo, Hokkaido, 060-8628, Japan*
**Corresponding author: yuki.shimizu@eng.hokudai.ac.jp*

Received XX Month XXXX; revised XX Month, XXXX; accepted XX Month XXXX; posted XX Month XXXX (Doc. ID XXXXX); published XX Month XXXX

A new method of generating interference patterns based on a non-orthogonal Lloyd's mirror interferometer with a spatial phase modulation is proposed. In the proposed method, a spatial light modulator (SLM) is introduced to a conventional non-orthogonal Lloyd's mirror interferometer so that arbitrary interference patterns, such as line interference patterns with varied line-spacing or two-dimensional patterns, can be generated by controlling the wavefronts of the laser beams at each position on the substrate. In this paper, as a first step of the research, the feasibility of the proposed method is theoretically confirmed by calculating interference patterns to be obtained when a spatial modulation of the phase delay is applied to the laser beams. A prototype of a non-orthogonal one-axis Lloyd's mirror interferometer with an SLM in its optical path is also designed and constructed. Some basic experiments are carried out to demonstrate the feasibility of the generation of interference patterns having varied line-spacing and two-dimensional patterns by the proposed method.

In the academic and industrial fields of precision machining and instrumentation, there is a constant demand for improved precision, and precision positioning technology is becoming increasingly important as an indispensable means of achieving this demand [1]. High-precision displacement sensors are essential to achieve high-precision positioning in such machine tools and measuring equipment. In such applications, displacement sensors such as laser interferometers, linear encoders, and capacitance displacement transducers are often employed [2–4]. In recent years, absolute linear encoders have been gaining a larger share of the market, especially in terms of throughput [1,5]. Recently, a method using a mode-locked femtosecond laser has also been proposed as an absolute linear encoder [6]; this method employs a diffraction grating with an unequally-spaced line pattern, which is often referred to as the varied (or variable) line-spacing (VLS) grating, as a scale for position measurement. A VLS grating is one of the key optical elements used in a wide range of scientific fields [7,8], and is gaining its importance.

The main methods for fabricating these VLS gratings include mechanical machining, direct writing by an electron beam (EB), and laser interference lithography [6,9,10]. In mechanical machining, VLS gratings are fabricated by adjusting the feed rate of the grating substrate relative to the cutting tool. In EB direct writing, it is possible to generate patterns with a higher resolution than that of mechanical machining. On the other hand, generating a grating pattern for a relatively wide area, such as the scale of a linear encoder, requires a large amount of time. In contrast, a method based on laser interference lithography can generate a wide range of grating patterns at high throughput by batch transfer of interference patterns. By deforming the substrate [11] or employing a concave mirror [12] in the interferometer, VLS gratings can be exposed. Adding curvature to the wavefront of the laser beam can also expose VLS gratings [13]. In the non-orthogonal Lloyd's mirror interferometer [14-17], which is the subject of this study, an example of generating unequally-spaced line patterns by inserting a concave lens into part of the optical path of the laser beam for the wavefront control has been demonstrated in experiments [6]. However, it has been difficult to freely adjust the pitch of the interference patterns with this method because the pitch depends on the focal length of the concave lens inserted. Therefore, it is expected to realize laser interference lithography in which the pitch can be adjusted more freely.

Regarding the background described above, in this paper, a method capable of generating arbitrary interference patterns, such as line interference patterns with VLS, is proposed by applying a spatial phase modulation with a spatial light modulator (SLM) [18,19] to a non-orthogonal Lloyd's mirror interferometer. Conventionally, the pitch of the interference patterns in the non-orthogonal Lloyd's mirror interferometer is adjusted by controlling the opening angle of the flat mirror reflector with respect to the substrate [14-17]. Since the laser beam is projected onto the substrate at a right angle, it is easy to apply additional optical systems to the interferometer. By utilizing the high scalability of the non-orthogonal Lloyd's mirror interferometer, in this paper, an attempt is made to generate line interference patterns with VLS and two-dimensional (2D) interference patterns by introducing an SLM in the optical path of the laser beam. As a first step of the research, the feasibility of the proposed method is confirmed by numerical calculations based on the theoretical equations. Also, a prototype optical system is designed and constructed, and basic experiments are carried out.

Principle. The basic diagrams of a proposed non-orthogonal Lloyd's mirror interferometer and phase delays given to the laser beam in the interferometer are shown in Figs. 1(a) and 1(b), respectively. Lloyd's mirror interferometer is a kind of wavefront-dividing type interferometer consisting of a substrate and a plane mirror reflector. Pattern exposure is performed by generating interference patterns by superimposing the laser beam directly incident on the substrate (sub-beam1) and that reflected by the mirror reflector (sub-beam2) on the substrate. In a conventional orthogonal Lloyd's-mirror interferometer, the mirror reflector is placed at 90° to the substrate, and the pitch of the interference pattern is adjusted by rotating the entire interferometer with respect to the laser beam [20]. On the other hand, in a non-orthogonal Lloyd's mirror interferometer, the mirror is positioned at an angle of 90°+α with respect to the substrate, while the laser beam is irradiated perpendicular to the substrate. The pitch g of the interference pattern is given by the following equation:

$$g = \lambda / \sin 2\alpha \,, \tag{1}$$

where λ is the wavelength of the laser beam. As can be seen in the equation, the pitch of the interference pattern can be adjusted by the angular position α of the mirror reflector. This optical configuration, in which the substrate is held stationary with respect to sub-beam1 during the alignment of the mirror reflector, has a feature that facilitates the introduction of additional optical systems. Taking this advantage, in this paper, an attempt is made to generate arbitrary interference patterns by introducing an SLM as an active device for the spatial phase modulation of the sub-beams.

Now we consider the case where the phase modulations ϕ_1 and ϕ_2 are given to the wavefronts of sub-beams 1 and 2, respectively. The light rays in sub-beams 1 and 2 incident at position $\boldsymbol{r}$=(X, Y, 0) on the substrate can be expressed as follows in complex amplitude form $\boldsymbol{E}_1(\boldsymbol{r})$ and $\boldsymbol{E}_2(\boldsymbol{r})$, respectively:

$$\boldsymbol{E}_1(\boldsymbol{r}) = E_1 \boldsymbol{e}_1 \exp\left(j\boldsymbol{k}_1 \cdot \boldsymbol{r} + \phi_0(\boldsymbol{r}) + \phi_1 \right), \tag{2}$$

$$\boldsymbol{E}_2(\boldsymbol{r}) = E_2 \boldsymbol{e}_2 \exp\left(j\boldsymbol{k}_2 \cdot \boldsymbol{r} + \phi_0(\boldsymbol{r}) + \phi_2 \right), \tag{3}$$

where E_i (i=1,2) is the amplitude of the electric field, $\boldsymbol{e}_i$ is the unit vector in the direction of polarization of the laser beam, and $\phi_0(\boldsymbol{r})$ is the initial phase of sub-beams. $\boldsymbol{k}_1$ and $\boldsymbol{k}_2$ are the wave vectors of the sub-beams 1 and 2, respectively, given as follows:

$$\boldsymbol{k}_1 = \frac{2\pi}{\lambda}(0, 0, -1),\, \boldsymbol{k}_2 = \frac{2\pi}{\lambda}(\sin 2\alpha, 0, -\cos 2\alpha). \tag{4}$$

Under the condition where the polarization directions of the sub-beams are the same ($\boldsymbol{e}_1$=$\boldsymbol{e}_2$), the light intensity distribution $I(\boldsymbol{r})$ of the interference pattern to be obtained by superposition of these light rays can be given by the following equation:

$$I(\boldsymbol{r}) = E_1^2 + E_2^2 + 2E_1E_2 \cos\left\{ (\boldsymbol{k}_1 - \boldsymbol{k}_2) \cdot \boldsymbol{r} + \phi_1 - \phi_2 \right\}. \tag{5}$$

As can be seen in the equation, by varying ϕ_1 and ϕ_2, the light

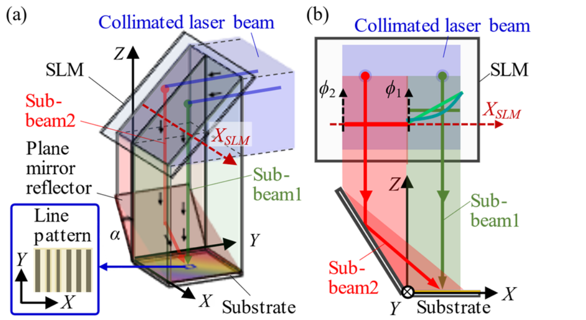

Fig. 1. (a) Basic diagrams of a non-orthogonal Lloyd's mirror interferometer with a spatial light modulator (SLM) and the (b) phase delays given to the sub-beams.

intensity of the interference pattern at position $\boldsymbol{r}$ can be adjusted. For example, in the case where no phase control is given to the entire sub-beam1 (ϕ_1=0) and a constant phase delay ϕ_C is given to the entire sub-beam2 (ϕ_2=ϕ_C), the line interference pattern with a constant pitch can be shifted in the X-direction. Also, in the case where a phase modulation that varies with position X is applied to sub-beams 1 or/and 2, a line interference pattern with a pitch that varies with location is expected to be obtained.

Based on the theoretical equations, the interference patterns to be obtained by a non-orthogonal one-axis Lloyd's mirror interferometer with a phase control are estimated by numerical calculations. It should be noted that the spatial resolution of an SLM is not considered in the numerical calculations. Now we assume a collimated laser beam from a laser source with a wavelength of λ=405 nm is employed as the laser beam for the generation of interference patterns. The opening angle α of the flat mirror reflector with respect to the substrate was set to 11.945°; in this case, from Eq (1), the pitch g of the line interference patterns to be obtained with no phase delay in the sub-beams (ϕ_1=ϕ_2=0) is calculated to be g=1.0 μm. Figure 2(a) shows the light intensity distribution of the line interference pattern to be obtained without wavefront control, calculated based on Eq (5). An equally-spaced line interference pattern with a pitch of 1 μm is estimated to be

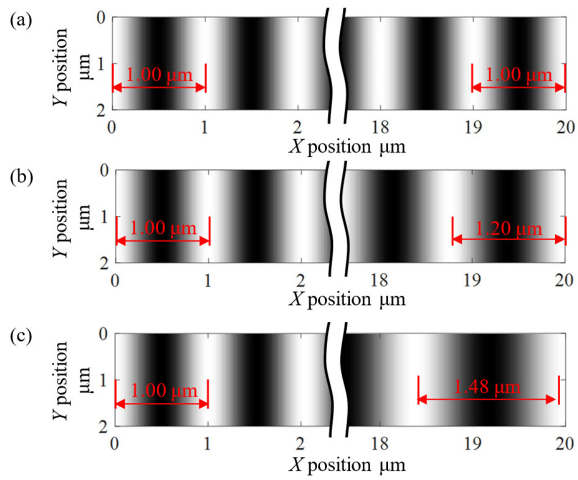

Fig. 2. Estimated line interference patterns when a is set to (a) zero, (b) 0.01π [rad/μm²] and (c) 0.02π [rad/μm²].

obtained. Numerical calculations are then extended to calculate the light intensity distribution of the line interference patterns to be obtained with the phase modulation. The light intensity distribution of the line interference patterns to be obtained in the case where a phase delay of $\phi_2=aX^2+bX+c$ is given to the wavefront of sub-beam2 is estimated. Figures 2(b), and 2(c) show the estimated line interference patterns to be obtained when b and c are set to zero and a is set to 0.01π and 0.02π [rad/μm^2], respectively. From these results, it is expected that the unequal pitch of the line interference patterns can be adjusted by the phase delay given to the wavefront of a sub-beam.

Experiments. To experimentally verify the feasibility of the proposed method, a prototype of the optical system was designed and constructed. Figure 3 shows a schematic diagram of the system. A laser diode with a light wavelength of 405.1 nm, a line width of less than 0.4 pm, and a power of 40 mW was employed as the laser source. This light source produced a laser beam with a diameter of 0.4 mm. The laser beam was made to pass through a spatial filter consisting of an objective lens and a pinhole, and was then collimated by using a collimating lens with a focal length of 100 mm to produce a laser beam with a diameter of approximately 9 mm. The generated laser beam was then made incident to an SLM (SLM-200, Santec AOC Corp., Japan) at an angle of incidence of 45°. The SLM had a pixel size of 7.8 μm square and a pitch of 8.0 μm. The phase delay on the wavefront could be controlled pixel by pixel with a resolution of 0.001π [rad]. Therefore, the phase delays of the wavefronts of sub-beams 1 and 2 could be controlled independently in the non-orthogonal one-axis Lloyd's mirror interferometer constructed in this study. Sub-beams 1 and 2 reflected by the SLM were then projected onto a non-orthogonal one-axis Lloyd's mirror interferometer. A flat mirror reflector with a flatness of $\lambda/10$ was employed in the interferometer, and was mounted on an $XY\theta_Z$ three-axis manual stage so that its position could be adjusted with respect to the substrate. It should be noted that a transparent glass substrate was employed in the setup so that the interference pattern can be observed from the backside. Taking advantage of the non-orthogonal setup that facilitates the introduction of additional optical systems, an optical microscope unit based on an infinity-corrected optical system with an objective lens having a focal length of 10 mm and NA of 0.42 was placed on the backside of the substrate [21].

Based on the constructed optical system, interference patterns were generated. At first, it was experimentally confirmed that interference patterns could be obtained even when the SLM was placed in the optical path of the laser beam. Figure 4(a) shows the interference patterns obtained by the developed interferometer when a plane mirror reflector was installed in place of the SLM in Fig. 3. As can be seen in the figure, line interference patterns with a constant pitch were obtained. Next, the mirror reflector was replaced by the SLM, and the interference patterns were generated without giving phase delays to the sub-beams ($\phi_1=\phi_2=0$). Figure 4(b) shows the result. Significant quality degradation of the generated line interference pattern was not found.

In the optical system constructed in this study, the laser beam is incident on the SLM at an oblique angle, so it is necessary to calibrate the relationship between the phase step given to the SLM and the amount of phase shift in advance. In this study, the phase step was varied to the SLM while a line interference pattern with a constant pitch was being produced, and the corresponding phase delay was calculated based on the amount of shift in the line interference pattern. The results are summarized in Fig. 5. In the following experiments, the phase delay given to the SLM was obtained based on this calibration result.

Next, an attempt was made to generate an interference pattern with an unequal pitch by adding a phase delay to sub-beam1 that varied from place to place on the substrate as shown in Fig. 6(a). Figure 6(b) shows the interference patterns obtained at each position on the substrate. From the observed line interference patterns, line pitches were evaluated. Figure 6(c) summarizes the results. In the figure, the pitches of the line interference patterns estimated based on theoretical equations are also plotted. As can be seen in the figure, the observed pitches are found to well agree with those calculated based on theoretical equations. From these results, it was experimentally demonstrated that the newly constructed optical system was capable of generating a line interference pattern whose pitch varies from place to place.

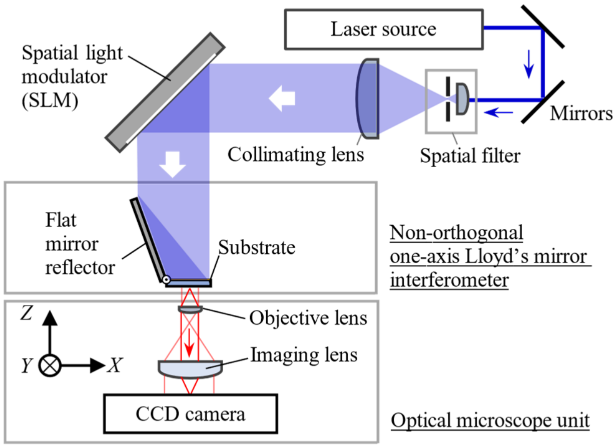

Fig. 3. Prototype optical setup of the non-orthogonal one-axis Lloyd's mirror interferometer with a spatial light modulator (SLM).

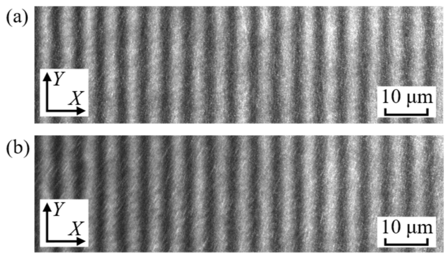

Fig. 4. Line interference fringes generated with sub-beam2 reflected by (a) a flat mirror reflector and (b) a spatial light modulator (SLM).

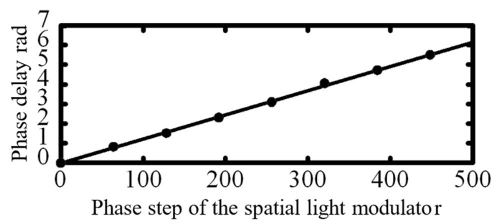

Fig. 5. Calibration result of the spatial light modulator (SLM).

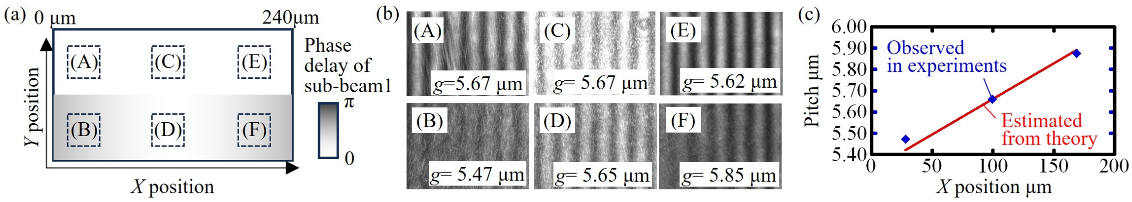

Fig. 6. Line interference fringes with unequal pitch generated by the developed optical setup, (a) Phase delay given to sub-beam1, (b) Observed line interference patterns, and (c) Pitch of the generated line interference pattern at each position.

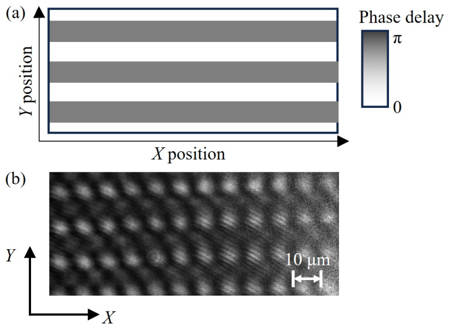

Fig. 7. (a) A phase delay applied to sub-beam1, and (b) obtained two-dimensional dot interference pattern.

Experiments were further extended to explore the possibilities of generating 2D interference patterns by the constructed optical system. Figure 7 shows the interference patterns obtained when a spatial phase modulation was applied to sub-beam1. The interferometer used in this study was a non-orthogonal one-axis Lloyd's mirror interferometer that conducts two-beam interference capable of generating line interference patterns. However, the experimental result demonstrated that 2D dot interference patterns can also be generated by adding a phase delay that varies in two in-plane directions to sub-beams by using the SLM. It should be noted that the pattern pitch was restricted by the pixel size of the SLM employed in the system. This is the first demonstration of the generation of 2D interference patterns by the developed system, and further detailed investigation on the 2D pattern formation capability of the system will be carried out in future work.

Conclusions. In this paper, an attempt has been made to introduce spatial wavefront modulation to a non-orthogonal Lloyd's mirror interferometer for the generation of line interference patterns with VLS and/or 2D patterns. By taking advantage of the high scalability of a non-orthogonal Lloyd's mirror interferometer, an SLM has successfully been integrated into the interferometer. The feasibility of controlling the interference patterns by adding a phase delay to the wavefronts of sub-beams has been demonstrated in experiments with the developed prototype of a non-orthogonal one-axis Lloyd's mirror interferometer.

In this paper, as a first step of the research, we have focused on finding the possibility of realizing active control of 2D interference patterns in a non-orthogonal one-axis Lloyd's mirror interferometer. The inventive and new aspect of the proposed approach is the spatial modulation of the phase delay, compared with the conventional Lloyd's mirror setup [17-20]. Also, the proposed setup allows the optical system to be configured by only one reflector, making operational adjustments much easier compared with the conventional two-axis Lloyd's mirror interferometer. Meanwhile, the spatial resolution of the phase delay to be added to the wavefronts of sub-beams depends on the pixel size of the employed SLM. Also, the realization of finer phase control over a wider area is an issue to be addressed and will be considered in future work.

Funding. JST, Fusion Oriented Research for Disruptive Science and Technology (FOREST), Japan (JPMJFR2027); the Japan Society for the Promotion of Sciences (JSPS) (22H01370); f^3 program in the Division of Mechanical and Aerospace Engineering, Hokkaido University, Japan.

Disclosures. The authors declare no conflicts of interest.

Data availability. Data underlying the results presented in this paper are not publicly available at this time but may be obtained from the authors upon reasonable request.

References

1. W. Gao, S. W. Kim, H. Bosse, *et al.*, CIRP Ann. Manuf. Technol. **64**, 773 (2015).
2. A. J. Fleming, Sens. Actuators A Phys. **190**, 106 (2013).
3. H. Schwenke, U. Neuschaefer-Rube, T. Pfeifer, *et al.*, CIRP Ann. Manuf. Technol. **51**, 685 (2002).
4. H. Kunzmann, T. Pfeifer, and J. Flügge, CIRP Ann. Manuf. Technol. **42**, 753 (1993).
5. Y. Altintas, A. Verl, C. Brecher, *et al.*, CIRP Ann. Manuf. Technol. **60**, 779 (2011).
6. Y. Shimizu, R. Ishizuka, K. Mano, *et al.*, Precis. Eng. **67**, 36 (2021).
7. S. Kim, J. Jin, Y.-J. Kim, *et al.*, Nature **453**, 757 (2008).
8. M. C. Hettrick and S. Bowyer, Appl. Opt. **22**, 3921 (1983).
9. C. Palmer and E. Loewen, DIFFRACTION GRATING HANDBOOK seventh edition (2014).
10. D. L. Voronov, E. M. Gullikson, and H. A. Padmore, Opt. Express **25**, 23334 (2017).
11. F. Bienert, T. Graf, and M. A. Ahmed, Opt. Express **31**, 5334 (2023).
12. H. Kim, H. Jung, D. H. Lee, *et al.*, Appl. Opt. **55**, 354 (2016).
13. A. Katzir, A. C. Livanos, J. B. Shellan, *et al.*, IEEE J. Quantum. Electron. **13**, 296 (1977).
14. Y. Shimizu, K. Mano, H. Murakami, *et al.*, 2019. Precis. Eng. **60**, 280 (2019).
15. Y. Shimizu, R. Aihara, K. Mano, *et al.*, Precis. Eng. **52**, 138 (2018).
16. Y. Cai, X. Li, R. Aihara, *et al.*, J. Adv. Mech. Des. Syst. Manuf. **10**, JAMDSM0080 (2016).
17. X. Li, W. Gao, Y. Shimizu, *et al.*, CIRP Ann. Manuf. Technol. **63**, 461 (2014).
18. N. Collings, W. A. Crossland, P. J. Ayliffe, *et al.*, Appl. Opt. **28**, 4740 (1989).
19. D. J. McKnight, D. G. Vass, and R. M. Sillitto, Appl. Opt. **28**, 4757 (1989).
20. P. F. Titchmarsh, Proceedings of the Physical Society **53**, 391 (1941).
21. N. Takahiro and Y. Shimizu, Int. J. Autom. Technol., in press (2023).

Full reference list (for review)

1. W. Gao, S. W. Kim, H. Bosse, H. Haitjema, Y. L. Chen, X. D. Lu, W. Knapp, A. Weckenmann, W. T. Estler, and H. Kunzmann, "Measurement technologies for precision positioning," CIRP Ann Manuf Technol **64**, 773 (2015).
2. A. J. Fleming, "A review of nanometer resolution position sensors: Operation and performance," Sens Actuators A Phys **190**, 106 (2013).
3. H. Schwenke, U. Neuschaefer-Rube, T. Pfeifer, and H. Kunzmann, "Optical methods for dimensional metrology in production engineering," CIRP Ann Manuf Technol **51**, 685 (2002).
4. H. Kunzmann, T. Pfeifer, and J. Flügge, "Scales vs. laser interferometers performance and comparison of two measuring systems" CIRP Annals **42**, 753 (1993).
5. Y. Altintas, A. Verl, C. Brecher, L. Uriarte, and G. Pritschow, "Machine tool feed drives," CIRP Annals **60**, 779 (2011).
6. Y. Shimizu, R. Ishizuka, K. Mano, Y. Kanda, H. Matsukuma, and W. Gao, "An absolute surface encoder with a planar scale grating of variable periods," Precis Eng **67**, 36 (2021).
7. S. Kim, J. Jin, Y.-J. Kim, I.-Y. Park, Y. Kim, and S.-W. Kim, "High-harmonic generation by resonant plasmon field enhancement," Nature **453**, 757 (2008).
8. M. C. Hettrick and S. Bowyer, Appl Opt **22**, 3921 (1983).
9. C. Palmer and E. Loewen, "DIFFRACTION GRATING HANDBOOK seventh edition", Newport Corporation (2014).
10. D. L. Voronov, E. M. Gullikson, and H. A. Padmore, "Large area nanoimprint enables ultra-precise x-ray diffraction gratings," Opt Express **25**, 23334 (2017).
11. F. Bienert, T. Graf, and M. A. Ahmed, "Theoretical investigation on the elimination of the period chirp by deliberate substrate deformations," Opt Express **31**, 5334 (2023).
12. H. Kim, H. Jung, D. H. Lee, K. B. Lee, and H. Jeon, "Period-chirped gratings fabricated by laser interference lithography with a concave Lloyd's mirror," Appl. Opt. **55**, 354 (2016).
13. A. Katzir, A. C. Livanos, J. B. Shellan, and A. Yariv, "Chirped gratings in integrated optics," IEEE J Quantum Electron **13**, 296 (1977).
14. Y. Shimizu, K. Mano, H. Murakami, S. Hirota, H. Matsukuma, and W. Gao, "Design optimization of a non-orthogonal two-axis Lloyd's mirror interferometer for fabrication of large-area two-dimensional scale gratings," Precision Engineering **60**, 280 (2019)
15. Y. Shimizu, R. Aihara, K. Mano, C. Chen, Y.L. Chen, X. Chen, and W. Gao, "Design and testing of a compact non-orthogonal two-axis Lloyd's mirror interferometer for fabrication of large-area two-dimensional scale gratings," Precision Engineering **52**, 138 (2018)
16. Y. Cai, X. Li, R. Aihara, R. Zongwei, Y. Shimizu, S. Ito, and W. Gao, "Investigation on the three-dimensional light intensity distribution of the fringe patterns generated by a modified two-axis Lloyd's mirror interferometer," Journal of Advanced Mechanical Design, Systems, and Manufacturing **10**, JAMDSM0080 (2016)
17. X. Li, W. Gao, Y. Shimizu, and S. Ito, "A two-axis Lloyd's mirror interferometer for fabrication of two-dimensional diffraction gratings," CIRP Annals **63**, 461 (2014).
18. N. Collings, W. A. Crossland, P. J. Ayliffe, D. G. Vass, and I. Underwood, "Evolutionary development of advanced liquid crystal spatial light modulators," Appl Opt **28**, 4740 (1989).
19. D. J. McKnight, D. G. Vass, and R. M. Sillitto, "Development of a spatial light modulator: a randomly addressed liquid-crystal-over-nMOS array," Appl Opt **28**, 4757 (1989).
20. P. F. Titchmarsh, "Lloyd's single-mirror interference fringes," Proceedings of the Physical Society **53**, 391 (1941).
21. N. Takahiro and Y. Shimizu, "A technique for estimating the pitch of interference fringe patterns for pattern exposure in a non-orthogonal one-axis Lloyd's mirror interferometer", International Journal of Automation Technology, in press (2023)